

Ab initio simulations for X-ray Thomson scattering

Contact j.vorberger@warwick.ac.uk

J. Vorberger, K. Wünsch and D. O. Gericke

Centre for Fusion, Space and Astrophysics, Department of Physics, University of Warwick, Coventry CV4 7AL, UK

Introduction

Over the last decade the frontier in experimental and theoretical physics has been pushed towards higher energies, higher densities and higher temperatures. An interesting part of this development is the investigation of high energy density and warm dense matter. The latter constitutes an intermediate state between high pressure solids/fluids and high density, high temperature plasmas. Naturally, such a state of matter is of high interest, since features known from solids or plasmas are combined and modified here. In addition, new physics may arise. Moreover, warm dense matter can be found in giant gas planets found in both our solar system and extrasolar systems, in brown dwarfs, and in other astrophysical objects^[1,2]. The development of the technologies for inertial confinement fusion as a future energy supply makes the warm dense matter state ever more important because the compression path crosses this region^[3,4].

These challenges led to a strongly enhanced interest in experimental studies of warm dense matter. One of the problems one faces immediately is the experimental characterization of the created states, that is, the measurement of density, temperature for electrons and ions, ionization degree, ionic and electronic structure, collective effects etc. Probing the deep interior of samples requires radiation with frequencies higher than the plasma frequency. Thus, one has to rely on X-rays for samples with solid density or above. Using powerful lasers, it has become possible to create such high-frequency probe beams and investigate warm dense matter in depth. The most promising method so far is X-ray Thomson scattering. Here, the radiation scatters off density fluctuations in the electron subsystem. The scattering spectrum contains information about the temperature, electron and mass densities, ionization state, as well as ionic and electronic structure^[5-8]. However, such measurement is not independent of theoretical models as those quantities are usually inferred by fitting a theoretical spectrum to the measured data. It is therefore of the utmost importance to provide a theoretical description of the scattering signal which is based on first principles. Based on structural information obtained from density functional molecular dynamics simulations (DFT-MD), such a description is presented in the following.

Theoretical scattering signal

The spectrum of the scattered radiation is directly proportional to the total electronic structure factor^[9-11]

$$\frac{d^2\sigma}{d\omega d\Omega} \propto S_{ee}^{tot}(k, \omega)$$

The electronic structure factor is the correlation function of density fluctuations in k-space. According to Chihara, it can be decomposed as follows^[9-11]

$$S_{ee}^{tot}(k, \omega) = [f(k) + q(k)]^2 S_{ii}(k) + Z_f S_{ee}^0(k, \omega) + Z_b \int d\omega' \tilde{S}^{ee}(k, \omega - \omega') S_s(k, \omega')$$

The first part describes the scattered signal from electrons co-moving with the ions, i.e., bound electrons accounted for by the form factor $f(k)$ and electrons in the screening cloud accounted for by the function $q(k)$. These electron density fluctuations are convoluted with the ion structure factor $S_{ii}(k)$. This ion feature can often be treated statically as the ion dynamics occurs on a longer time scale and cannot be resolved in most laser-experiments. The second summand describes contributions from free electrons which are usually weakly coupled. This free electron term has to be treated dynamically; it gives rise to collective excitations like plasmons. Analysis of the screening function $q(k)$ shows that the distinction between electrons being in the screening cloud contributing to the ion peak and electrons contributing to the free electron part is somewhat arbitrary. The third term accounts for bound-free transitions and internal excitations.

The Chihara formula is based on an artificial division of the electrons into bound and free. This is equivalent to performing a transition from the physical picture (only electrons and nuclei as elementary particles) to the chemical picture (free electrons and ions of different charge state as elementary particles). First principle simulations do not allow such a division into bound and free states. For the ion part of the total electron structure factor, we therefore propose to introduce a single density comprising bound and screening (free) electrons^[12]

$$W_R(k) = [f(k) + q(k)]^2 S_{ii}(k) \Rightarrow n_e^2(k) S_{ii}(k).$$

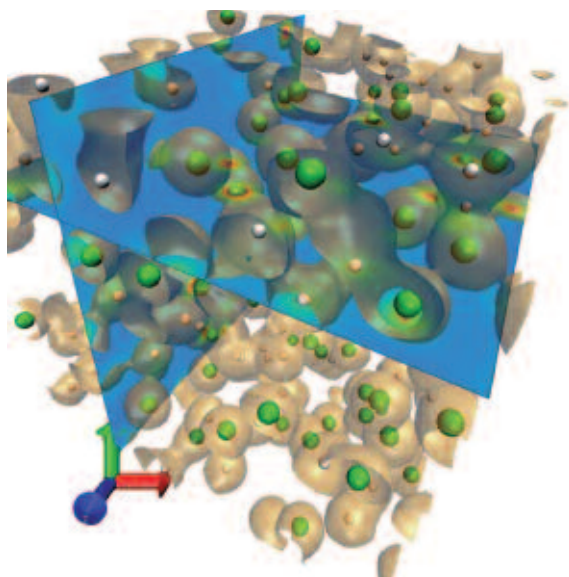


Figure 1. Snapshot of a simulation of LiH at 2.25 g/cc and 2.2 eV. Lithium nuclei are depicted as green spheres, hydrogen nuclei are white. An isosurface of the electron density is plotted in orange. In addition, two 2-D slices of the electron density are shown.

Ab initio simulations

The advantage of so called ab initio simulations is clearly the fact that they start from a small set of basic physical formulas to describe the complex physical situation. However, no first principle calculation is completely without approximation. In density functional molecular dynamic simulations (DFT-MD), controlled and uncontrolled approximation are existent. Such approximations as system size (number of electrons and ions), step size in time, run time, k-point sampling, pseudo-potentials used etc. are controllable, i.e., these parameters can be checked for convergence. The Kohn-Sham Ansatz to represent the many body wave function of the electrons by one particle wave functions and to describe electron-electron correlations by an exchange correlation functional is an uncontrolled approximation. Still, even a perfect ab initio simulation able to compute the exact total electron structure factor would not solve the problem of understanding the system. It is better thought of as a numerical experiment which still needed a division of the total electron structure factor according to Chihara to understand the physical processes in the system and to interpret the scattering signal. Thus, the task is two-fold: perform the best ab initio simulations and extract as much information as possible so as to match these quantities with those in the Chihara formula. When attempting this, a further difficulty arises: the experiments are conducted at specific conditions of temperature and density which are unknown and are to be determined when analyzing the scattering spectrum.

Ab initio simulations rely on input values for temperature and density to produce an artificial, theoretical scattering spectrum. Only by adjusting a theoretical scattering spectrum to the measured one, the conditions of temperature and density needed can be fixed. We are therefore forced to perform a self consistency cycle between experimental and theoretical

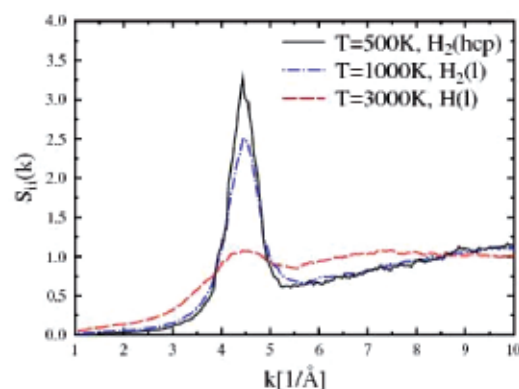


Figure 2. Structure factor for warm dense hydrogen at $P = 138$ GPa (0.8 g/cc) in three different phases: solid molecular (black solid line), fluid molecular (blue dash-dotted line), and metallic fluid (red dashed line).

data. However, first principle simulations are highly demanding on computer power and time. Thus they seem to be inapplicable for this task. Faster methods, usually in the chemical picture, with far cruder approximation are therefore used to extract temperature and density data from the experimental spectrum. In general, these methods do not give similar results for the electronic and ionic structure as the ones that follows from first principle calculations. Accordingly, ab initio simulations are often used to produce theoretical spectra using temperature and density data that are not consistent. Consequently, a third task for ab initio simulation is to identify those simple models that reproduce its results.

We use DFT-MD to describe warm dense matter as studied in recent experiments: we performed simulations for aluminium, lithium, beryllium, hydrogen, carbon, plastic (CH), and lithium hydride (LiH). For this purpose we use the program packages VASP, CPMD, and abinit^[13-17]. Those are plane wave DFT-MD codes employing electron-ion pseudo-potentials for higher efficiency. These pseudo-potentials are usually chosen to include all electrons, except for carbon where the inner s-shell is treated as core. VASP is able to use the projector augmented wave method (PAW) to always treat all electrons explicitly^[13]. System sizes are from 128 up to 1024 nuclei with the according number of electrons. The ion temperature can be established as in a canonical ensemble by employing a Nose-Hoover thermostat. Average temperature effects of the electrons are accounted for by using a real temperature Fermi distribution to populate the eigenstates. For fluid like matter integrations over the Brillouin zone can usually be reduced to the Gamma point only.

Results and discussion

A typical snapshot of a DFT-MD simulation is shown in Fig. 1. The only useful information such a picture provides is that the ion ordering is random as in a fluid and that some electron density remains centered at the ion positions. However, the ion structure factor and the electron-ion distribution can be extracted from such snapshots. Fig. 2 shows a typical example for hydrogen which is especially instructing as changes from the solid molecular phase to the fluid molecular

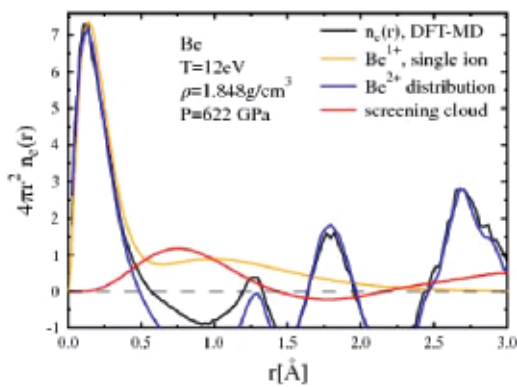


Figure 3. Electron distribution around an ion for warm dense beryllium. The black line is the density distribution as extracted from DFT-MD. The yellow line is the electron density for a single charged ion in vacuum. The blue line arises when every ion position in the simulation box receives the unperturbed electron distribution of a doubly charged ion. The red line is the screening cloud as extracted as difference between black and blue line. The uniform free electron density has been subtracted for the black and blue lines.

phase and finally the fluid metallic phase can clearly be resolved. Results for the ionic structure in other light elements such as beryllium and lithium can be found in Ref. [18].

Similarly, one may plot the distribution of the electron density around an ion. Fig. 3 presents an example for beryllium. In this way, it is possible to analyze the influence of the surrounding medium on the bound states. In the case of Fig. 3, the 2s shell of beryllium is completely ionized. On the other hand, the inner 1s shell is unaffected from temperature ionisation. Furthermore, temperature alone could not have ionised two electrons which is indeed an effect of the high density of solid beryllium (pressure ionisation). For distances larger than half an Angstrom, further electron density maxima can be observed at the positions of the neighboring ions. In addition, the local electron density is depleted compared to the average electron density in areas where $4\pi r^2 n(r)$ is negative as the mean electron density was subtracted.

The electron density in k -space and the ion structure factor may be combined into a prediction for the ion feature of the total electron structure factor, the weight of the Rayleigh peak $W_R(k)$ – see Fig. 4. Starting from high wave vector values, the DFT-MD data reproduce the correct limit for doubly ionized beryllium ions. This is in agreement with the behavior seen in Fig. 3 for small distances. For intermediate and small wave vectors we see a lowering of the ion feature culminating in the development of a maximum and subsequently a strong decrease in magnitude. This

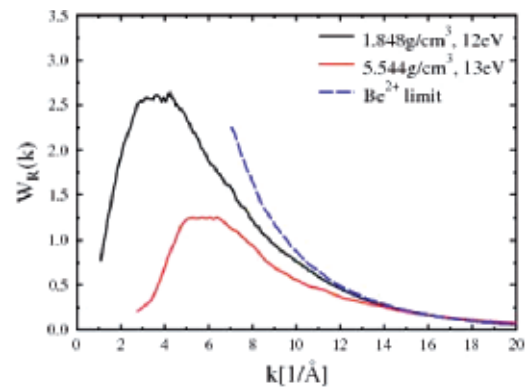


Figure 4. Weight of the Rayleigh Peak $W_R(k)$ for beryllium at normal density (1.848 g/cc) and threefold compressed (5.544 g/cc) as obtained from DFT-MD. The high k limit of doubly ionized beryllium ions is shown as blue dashed line.

behavior is partly due to the ion structure factor, which shows the typical correlation hole for small wave vectors. The drastic decrease for small wave vectors can however be attributed to correlation effects in the electronic density around the ions. The electronic density $n(k)$ is reduced as compared to ideal form factors and screening clouds which do not include the effects of the surrounding medium of further ions and electrons.

Comparison with experiment and simple models

Comparison of our theoretical spectra with experimental values is promising so far. However, agreement is not consistent over the whole range of temperature, density and material. For Beryllium at solid density and some electron volts experimental and theoretical weight of the Rayleigh peak agree very well [12]. Also, the experimentally obtained structure factor for shock-compressed lithium is in agreement with simulations [7].

We have been able to establish that the ion structure as obtained with DFT-MD is best reproduced by employing a simple linearly screened one component plasma model for the ions. Attempts to map the full electron-ion system onto a classical description by the use of weak electron-ion pseudo-potentials were futile [18,19]. Deviations from the simple linear screening law can be important in cases where interactions between closed inner electron shells become important. In such circumstances, a Lennard-Jones type soft core repulsion potential can in addition be fitted to improve agreement [18].

Acknowledgements

This work was supported by the UK Engineering and Physical Sciences Research Council.

References

1. B. Militzer, J. Vorberger, I. Tamblyn, S. A. Bonev, W. B. Hubbard, *ApJ* **688**, L45 (2008).
2. N. Nettelman *et al.*, *ApJ* **683**, 1217 (2008).
3. J. D. Lindl *et al.*, *Phys. Plasmas* **11**, 339 (2004).
4. A. Grinenko, D. O. Gericke, S. H. Glenzer, J. Vorberger, *Phys. Rev. Letters* **101**, 194801 (2008).
5. S. H. Glenzer *et al.*, *Phys. Rev. Lett.* **90**, 175002 (2003).
6. S. H. Glenzer *et al.*, *Phys. Rev. Lett.* **98**, 065002 (2007).
7. E. Garcia Saiz *et al.*, *Nature Physics* **4**, 940 (2008).
8. A. L. Kritcher *et al.*, *Science* **322**, 69 (2008).
9. J. Chihara, *J. Phys. Cond. Matt.* **12**, 231 (2000).
10. G. Gregori *et al.*, *Phys. Rev. E* **67**, 026412 (2003).
11. G. Gregori *et al.*, *Phys. Plasmas* **11**, 2754 (2004).
12. J. Vorberger *et al.*, submitted to *Phys. Rev. Lett.*
13. G. Kresse, J. Hafner, *Phys. Rev. B* **49**, 14251 (1994).
14. G. Kresse and J. Furthmüller, *Phys. Rev. B* **54**, 11169 (1996).
15. P. E. Blöchl, *Phys. Rev. B* **50**, 17953 (1994).
16. X. Gonze *et al.*, *Comp. Mat. Science* **25**, 478 (2002).
17. CPMD consortium, IBM Corp, MPI Stuttgart
18. K. Wünsch, J. Vorberger, and D. O. Gericke, *Phys. Rev. E* **79**, 010201(R) (2009).
19. K. Wünsch, P. Hilse, M. Schlanges, D. O. Gericke, *Phys.* **77**, 056404 (2008).